Eur. Phys. J. E (2012) **35**: 90
DOI 10.1140/epje/i2012-12090-1

THE EUROPEAN PHYSICAL JOURNAL E

Regular Article

On the occurrence of polygon-shaped patterns in vibrated cylindrical granular beds

G. Lu[a], J.R. Third, M.H. Köhl, and C.R. Müller[b]

ETH Zürich, Leonhardstrasse 27, 8092 Zürich, Switzerland

Received 26 July 2012
Published online: 25 September 2012 –

Abstract. We report experimental observations of polygon-shaped patterns formed in a vertically vibrated bed of circular cross-section. A phase map is determined, showing that the polygon pattern is established for $\Gamma = A(2\pi f)^2/g \gtrsim 10$. The sensitivity of the polygon structure to bed parameters was tested by studying beds of different particle sizes and fill levels. It was hypothesized that the polygon pattern observed in cylindrical beds is the corresponding pattern to the formation of arches in square-shaped beds. The close relationship between these two patterns was demonstrated by two observations: i) the radii of the arches of a corresponding square bed and the inner radius of the cylindrical bed were found to be very similar and ii) the boundary lengths of the two patterns were in good agreement.

Granular systems are assemblies of macroscopic particles, which under external excitation, *e.g.* rotation or vibration, can display a plethora of intriguing phenomena including segregation or the formation of surface waves [1–4]. In particular, the different structures formed if a bed of particles is vibrated have attracted significant attention [5–12]. As an example, if a monolayer of spherical beads is excited by vertical vibrations of a large vibrational amplitude, the grains behave like a gas. Upon cooling of the system, *i.e.* reducing the amplitude of the vibrations, clusters of particles are observed to coexist with the granular gas [13]. In addition, for quasi-2D vibrated beds that contain multiple layers of spherical beads, heaping is observed due to the so-called block-slip-motion at the walls [14]. The formation of patterns of sub-harmonic undulations, *e.g.* arching and surface waves, have also been demonstrated in quasi-2D beds [15,16]. Fine particles (*e.g.* diameter 0.2 mm) vibrated vertically in 3D beds revealed a plethora of well-defined surface structures. Depending on the vibrational acceleration, strips, hexagons, kinks, squares and localized oscillations, so-called oscillons, were observed [17–19]. Recently, patterns formed in beds composed of non-spherical particles have received considerable attention. In vibrated beds containing long rods, it was found that the large aspect ratio of the particles induced a dense, highly ordered, crystalline state, *viz.* the rods aligned vertically to form clusters [20, 21]. Subsequently, it was observed that such clusters undergo collective motion in the form of vortices [22,23]. In addition, a vibrated monolayer of long rods showed large density fluctuations, probably arising from curvature induced currents [24, 25].

So far, most studies concerned with the dynamics of 2D vibrated beds have only considered beds of rectangular geometries. Only very little attention has been paid to the effect of the shape of the vessel containing the granular material on the particle dynamics. However, it has been reported that the convection pattern and, thus, the segregation behavior reverses when the shape of a 3D vibrated bed was changed from a cylinder to a cone [26]. This work is concerned with the motion of particles within a quasi-2D vibrated bed of circular cross-section. In this geometry, we report new patterns and demonstrate how these patterns are related to the arching structure which has been observed previously in quasi-2D beds of rectangular cross-section [27].

Experimental measurements were first performed in a quasi-2D bed comprising a brass cylinder of internal diameter 110 mm and thickness 9 mm with two sheets of anti-static Perspex being placed at its front and rear. A small orifice at the top of the cylinder allowed particles to be added or removed from the bed. The bed was bolted onto an electrodynamic shaker (Labworks Inc., ET-139). A controller (Labworks Inc., VL-144), amplifier (Labworks Inc., PA-138-1) and accelerometer (PCB Piezotronics Inc., $J352C33$) were used to generate regular, sinusoidal oscillations. Spherical glass beads of density 2.5 g/cm^2 (Sigmund Lindner, Germany) were used as the granular material. The particles were imaged using a high-speed CCD camera (Nikon, $496RC2$). In this work the filling height of the bed, H, is defined as the height of the material above the lowest point of the cylindrical

[a] e-mail: lugu@student.ethz.ch
[b] e-mail: muelchri@ethz.ch

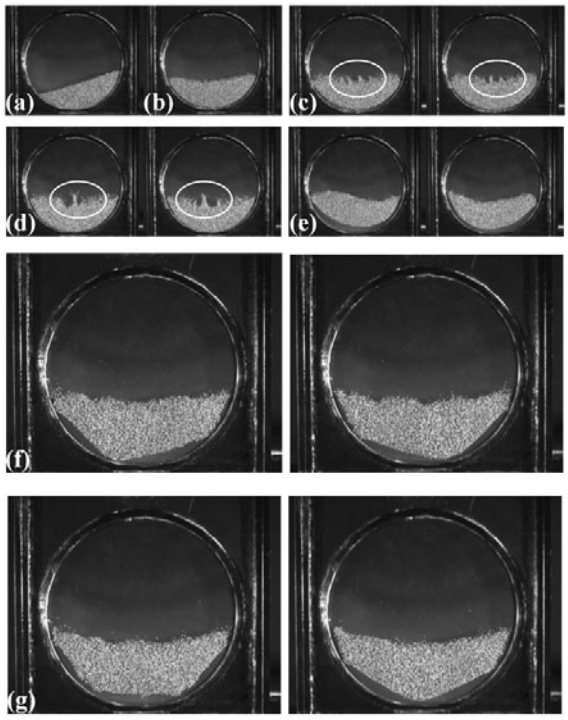

Fig. 1. Snapshots of granular patterns observed in a quasi-2D, cylindrical vibrated bed (particle diameter 0.5–0.75 mm; fill level 1/4): (a) Faraday tilting ($f = 18$ Hz, $\Gamma = 2.0$), (b) symmetric convection pattern ($f = 18$ Hz, $\Gamma = 3.3$), (c) $1/2f$ surface waves ($f = 15$ Hz, $\Gamma = 3.6$), (d) $1/4f$ surface waves ($f = 26$ Hz, $\Gamma = 6.8$), (e) kinks ($f = 25$ Hz, $\Gamma = 8.8$), (f) polygon mode 1, *i.e.* non-symmetric about the central plane of the bed ($f = 35$ Hz, $\Gamma = 12.3$), and (g) polygon mode 2, *i.e.* symmetric about the central plane of the bed ($f = 40$ Hz, $\Gamma = 19.3$).

wall. The fill level, h, is defined as the ratio of the filling height to the internal diameter of the cylinder.

First a bed of fill level $h = 1/4$ containing spheres with diameters in the size range of 0.5–0.75 mm was studied. Depending on the value of the dimensionless acceleration, $\Gamma = A(2\pi f)^2/g$, where A and f are the amplitude and frequency of the vibration, respectively, a variety of well-defined granular patterns were observed. Snapshots of these patterns are shown in fig. 1 and a phase map that correlates the occurrence of each pattern with Γ and f is shown in fig. 2. For $1 \lesssim \Gamma \lesssim 3$, a convection pattern is established, *i.e.* particles are transported in an ordered fashion within the bulk of the material, and for $\Gamma \lesssim 2$ Faraday tilting prevails [28]. Here, particles roll down at the surface of the bed and are transported back to the top of the bed inside the bulk. Increasing Γ to ≈ 2, the surface of the bed becomes horizontal. At this stage, the convection pattern is dominated by particles moving downward in the center and moving upward close to the walls, similar to the particle flow within a vibrated conical container [26]. Increasing Γ further to ≈ 3 weakens the convection. Indeed, the bed starts to detach from the bottom of the wall during most of the oscillation cycle, resulting in the formation of surface waves. This regime can be split into

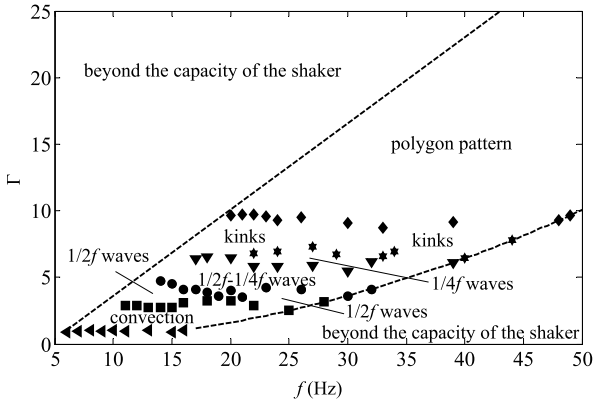

Fig. 2. Phase map of patterns formed in a quasi-2D, cylindrical vibrated bed (particle diameter 0.5–0.75 mm; fill level $h = 1/4$).

three sub-regimes depending on the frequency of the surface waves: $1/2f$ and $1/4f$ surface waves are formed for Γ in the range of 3–4.5 and 6.5–7, respectively. Between these two regimes a transition zone is observed. However, these patterns are not as clearly defined as they are in rectangular beds and the waves were only found to form in the central part of the bed surface.

Increasing Γ further to about 7.5 leads to the formation of kinks, *viz.* neighboring sections of the bed oscillate out of phase. Starting from $\Gamma \approx 10$, we observed a new pattern, which has never been reported previously, *viz.* the formation of a polygon structure. The free surface of the bed is fairly flat with no evident surface waves, while the bottom of the bed clearly shows vertices and edges, giving rise to a polygon inscribed within the cylindrical wall. Once a vertex of the polygon impacts with the curved wall, the particles colliding with the wall move sideways in opposite directions, away from the original vertex. Thus, a new vertex forms when particle flows originally moving in opposite directions from two neighboring vertices meet. Typically, in the polygons formed, the lengths of the polygon edges are different. Close to the bottom of the bed the edges are longer compared to the edges generated higher up in the bed. For the case that a symmetric polygon is formed (fig. 1(g)), the two symmetric edges are, of course, of equal length. However, it is worth mentioning that we found no clear relationship between the formation of a symmetric polygon and Γ. For the case of a symmetric polygon, the number of edges was occasionally observed to increase or decrease in successive oscillation cycles. The maximum and the minimum number of edges observed were, respectively, 6 and 3.

Changing to particles with a size range of 0.3–0.4 mm while keeping a fill level of $h = 1/4$, the patterns observed previously still occurred. However, the formation of surface waves was almost impossible to identify. Nonetheless, we could still observe two different modes of polygon formation, *i.e.* polygons with or without symmetry with respect to the central plane of the bed. In order to test the sensitivity of the formation of the polygon pattern to further bed parameters, beds with a fill level of $h = 1/2$

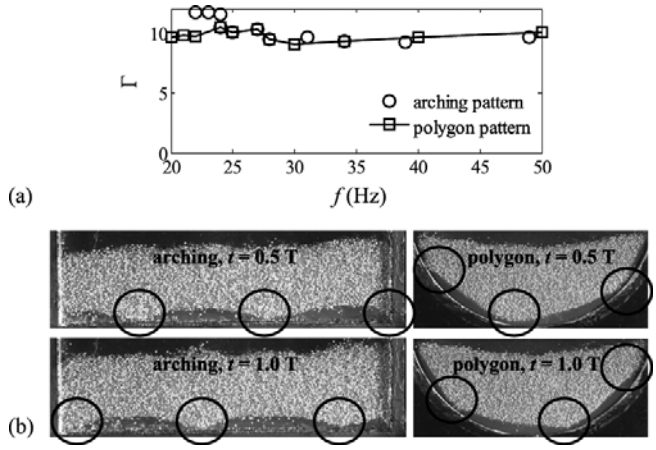

Fig. 3. Comparison of the characteristics of the polygon and arching patterns: (a) The transition from kinks to the arching or the polygon patterns formed within either a square-shaped or cylinder-shaped bed. (b) Snapshots of the arching and the polygon patterns formed at $f = 50$ Hz and $\Gamma = 20.1$ (the circles highlight the positions of the nodes formed).

were studied for both particle sizes, *i.e.* 0.5–0.75 mm and 0.3–0.4 mm. For particles of diameter 0.5–0.75 mm no polygon regime was observed in the tested (Γ, f)-space. On the other hand, for particles of diameter 0.3–0.4 mm the polygon structure was still observable and its location on the phase map was very similar to that using a fill level of $h = 1/4$, *i.e.* $\Gamma \gtrsim 8$. However, contrary to our expectations, the number of polygon edges did not increase with fill level. For a fill level of $h = 1/2$, the locations of straight edges and sharp vertices were constrained to the bottom section of the bed, while the upper region of the bed remained curved, following the curvature of the periphery of the cylindrical wall.

The phase map plotted in fig. 2 suggests that there might be a connection between the polygon structure observed in a cylindrical bed and the arching pattern observed in beds of rectangular cross-section, since both patterns occur at high values of Γ [27]. In addition, for both patterns the top surface of the bed is relatively flat with no evident waves, while the bottom of the bed shows either straight edges or curved arches. We speculated that the curvature of the arches with respect to the flat wall is compensated by the curvature of the cylindrical wall, thus leading to straight edges. In order to validate this assumption, we used the previous cylindrical bed filled with particles of diameter 0.5–0.75 mm to give a fill level of $h = 1/4$. In addition, two square beds were constructed. The length of the first bed, $L_1 = 115$ mm, corresponded to the circumference of the section of the cylindrical wall that is covered by particles for a fill level of $h = 1/4$. The length of the second bed, $L_2 = 95$ mm, was equal to the projection of the circumference of the section of the cylindrical wall that is covered by particles for a fill level of $h = 1/4$ onto a horizontal plane. The spacing between the front and the rear wall was equal to the thickness of the cylindrical bed (9 mm). Thus, different filling heights were obtained when the same volume of the particles was

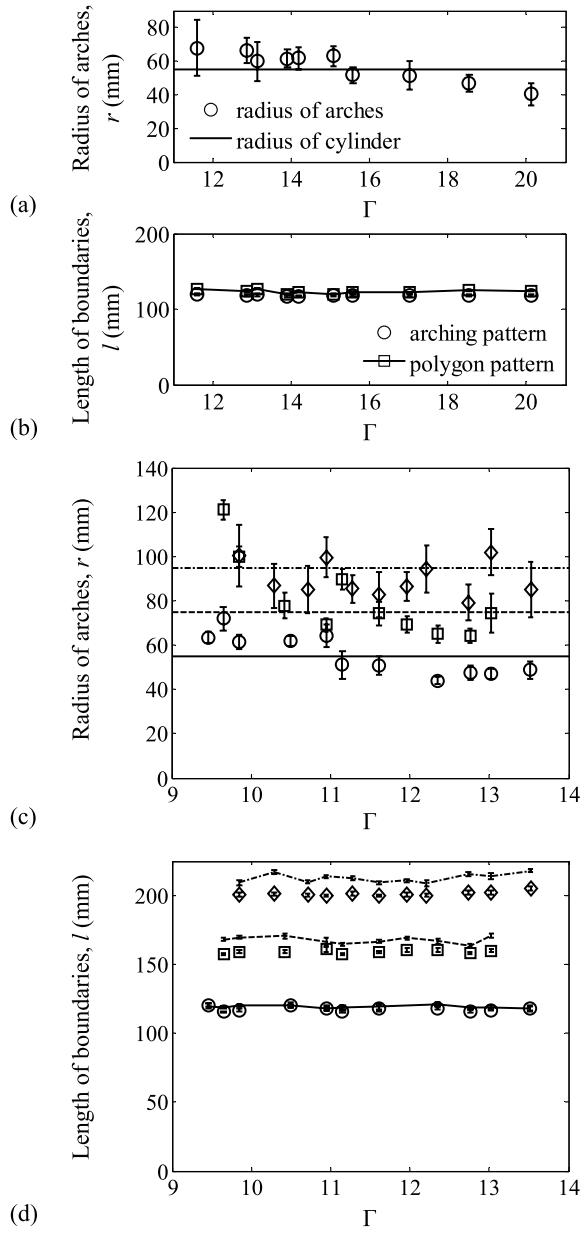

Fig. 4. Comparison of the characteristics of the polygon and arching patterns (in figs. 4(c) and (d) the following symbols are used: (◯) L_{s1}, (□) L_{s2}, (◇) L_{s3}, (−) R_1, (− − −) R_2, (− · −) R_3): (a) Comparison between the radii of the arches and the radius of the brass cylindrical bed; (b) comparison between the lengths of the boundaries of the polygon (using the brass cylindrical bed) and the arching patterns; (c) comparison between the radii of the arches and the radii of the PMMA-made cylindrical beds of different dimensions; and (d) comparison between the lengths of the boundaries of the polygon (using the PMMA-made cylindrical beds) and the arching patterns.

poured into the two square beds, *i.e.* $H_1 = 20$ mm for the bed of length L_1 and $H_2 = 26$ mm for the bed of length L_2.

To determine which square bed design is the best representation of a cylindrical bed of fill level $h = 1/4$, we investigated the transition from kinks to the arching patterns in the square beds. As shown in fig. 3(a), for the

bed of length L_1, the transition from kinks to the arching pattern matched well the transition from kinks to the polygon pattern in the vibrated cylindrical bed for the (Γ, f)-space studied. On the other hand, for the bed of length L_2, no arching pattern could be observed in the whole (Γ, f)-space tested. Thus, with regards to pattern formation, it appears that the square bed of length L_1 provided a better representation of a cylindrical bed of fill level $h = 1/4$. Figure 3(b) further shows a typical set of snapshots obtained from these two systems. Both patterns are centrally non-symmetric and are mirrored about the central plane of the bed during subsequent vibrating cycles.

In order to evaluate further the relationship between the polygon and arching patterns, two additional experiments were performed. First, we used the square bed ($L_1 = 115$ mm) and measured the radii of the arches formed, which were anticipated to be close to the inner radius of the cylindrical bed (55 mm). For this study, A ranged between 1.5 mm and 3 mm and f was varied between 31 Hz to 50 Hz. Note that only images capturing the fully developed patterns were employed. The fully developed states were defined as the moment when the bed as a whole reaches the highest position relative to the container itself. For such images only complete arches were chosen. The radii of the arches were averaged over 1 s of measurement for each Γ (approximately 30–75 arches per Γ), and the results are plotted in fig. 4(a) as a function of Γ. It can be seen that for Γ ranging from 13 to 19, the arch radii determined were in close agreement with the inner radius of the cylindrical bed (55 mm). Additionally, we compared the boundary length of both the polygon pattern (*i.e.* the edge length) and the arching structure (*i.e.* the length of the curved segment). In fig. 4(b), the boundary lengths determined are plotted as a function of Γ. For both patterns the boundary lengths were in close agreement and also independent of Γ.

Finally, to support further the hypothesis that the formation of polygon patterns in cylindrical beds is the geometrical equivalent of the formation of arching structures in square beds, the radii of the arches and the boundary length of both patterns were determined in additional cylinder-shaped beds and square-shaped beds of different dimensions. The beds were constructed of PMMA and the spacing between the front and the rear wall was set to 15 mm. The inner radii of the additional cylindrical beds were $R_1 = 55$ mm, $R_2 = 75$ mm and $R_3 = 95$ mm. A fill level of $h = 1/4$ was used for each bed, resulting in the following lengths of the corresponding square-shaped beds: $L_{s1} = 115$ mm, $L_{s2} = 157$ mm and $L_{s3} = 199$ mm, respectively. The filling heights of these three square beds were, thus, $H_{s1} = 17$ mm, $H_{s2} = 22$ mm and $H_{s3} = 29$ mm, respectively. In figs. 4(c) and (d), the experimentally determined radii of the arches and the length of the pattern boundaries are plotted as a function of Γ. Again, the radii of the arches are in close agreement with the inner radius of the cylindrical beds. Also, the boundary lengths of both patterns are, as previously observed, independent of Γ and in close agreement with each other.

To summarize, a previously unreported polygon-shaped pattern, formed in a vertically vibrated quasi-2D cylindrical bed, is reported. We propose that the polygons formed inside a cylinder-shaped bed are a geometrical transformation of the arching structure typically encountered in square-shaped vibrated beds. Evaluation of characteristics of the patterns, such as the radii of the arches and the lengths of the polygon and arching boundaries, confirmed the close relationship between the two patterns.

The authors are grateful to the Swiss National Science Foundation (Grant 200021_132657/1) and the China Scholarship Council (Guang Lu) for partial financial support of this work.

References

1. H.M. Jaeger, S.R. Nagel, R.P. Behringer, Rev. Mod. Phys. **68**, 1259 (1996).
2. I.S. Aranson, L.S. Tsimring, Rev. Mod. Phys. **78**, 641 (2006).
3. J.M. Ottino, D.V. Khakhar, Annu. Rev. Fluid Mech. **32**, 55 (2000).
4. G. Seiden, P.J. Thomas, Rev. Mod. Phys. **83**, 1323 (2011).
5. Z.H. Jiang, Y.Y. Wang, J. Wu, Europhys. Lett. **74**, 417 (2006).
6. P.F. Stadelr, J.M. Luck, A. Mehta, Europhys. Lett. **57**, 46 (2001).
7. P.M. Reis, G. Ehrhardt, A. Stephenson, T. Mullin, Europhys. Lett. **66**, 357 (2004).
8. C.P. Clement, H.A. Pacheco-martinez, M.R. Swift, P.J. King, Europhys. Lett. **91**, 54001 (2010).
9. L. Trujillo, M. Alam, H.J. Herrmann, Europhys. Lett. **64**, 190 (2003).
10. M. Bose, P.R. Nott, V. Kumaran, Europhys. Lett. **68**, 508 (2004).
11. G. Gutiérrez, O. Pozo, L.I. Reyes, V.R. Paredes, J.F. Draek, E. Ott, Europhys. Lett. **67**, 369 (2004).
12. D.A. Sanders, M.R. Swift, R.M. Bowley, P.J. King, Europhys. Lett. **73**, 349 (2006).
13. J.S. Olafsen, J.S. Urbach, Phys. Rev. Lett. **81**, 4369 (1998).
14. E. Clement, J. Duran, J. Rajchenbach, Phys. Rev. Lett. **69**, 1189 (1992).
15. C.R. Wassgren, C.E. Brennen, M.L. Hunt, J. Appl. Mech. **63**, 712 (1996).
16. O. Sano, Phys. Rev. E **72**, 051302 (2005).
17. F. Melo, P.B. Umbanhowar, H.L. Swinney, Phys. Rev. Lett. **75**, 3838 (1995).
18. P.B. Umbanhowar, F. Melo, H.L. Swinney, Nature **382**, 793 (1996).
19. C. Bizon, M.D. Shattuck, J.B. Swift, W.D. Mccormick, H.L. Swinney, Phys. Rev. Lett. **80**, 57 (1998).
20. F.X. Villarruel, B.E. Lauderdale, D.M. Mueth, H.M. Jaeger, Phys. Rev. E **61**, 6914 (2000).
21. V. Narayan, N. Menon, S. Ramaswamy, J. Stat. Mech. **01**, P01005 (2006).
22. D.L. Blair, T. Neicu, A. Kudrolli, Phys. Rev. E **67**, 031303 (2003).
23. I.S. Aranson, D. Volfson, L.S. Tsimring, Phys. Rev. E **75**, 051301 (2007).

24. V. Narayan, S. Ramaswamy, N. Menon, Science **317**, 105 (2007).
25. V. Narayan, S. Ramaswamy, N. Menon, Science **320**, 612 (2008).
26. J.B. Knight, H.M. Jaeger, S.R. Nagel, Phys. Rev. Lett. **70**, 3728 (1993).
27. S. Douady, S. Fauve, C. Laroche, Europhys. Lett. **8**, 621 (1989).
28. R.J. Milburn, M.A. Naylor, A.J. Smith, M.C. Leaper, K. Good, M.R. Swift, P.J. King, Phys. Rev. E **71**, 011308 (2005).